ELSEVIER

Journal of Nuclear Materials 307–311 (2002) 1424–1429

journal of nuclear materials

www.elsevier.com/locate/jnucmat

Helium and tritium kinetics in irradiated beryllium pebbles

E. Rabaglino [a,b,*], J.P. Hiernaut [b], C. Ronchi [b], F. Scaffidi-Argentina [a,c]

[a] *Forschungszentrum Karlsruhe, Institute for Nuclear and Energy Technologies, P.O. Box 3640, 76021 Karlsruhe, Germany*
[b] *European Commission, Joint Research Centre, Institute for Transuranium Elements, P.O. Box 2340, D-76125 Karlsruhe, Germany*
[c] *Culham Science Centre, EFDA Close Support Unit Culham, Abingdon, Oxon OX14 3DB, UK*

Abstract

High-precision measurements of the release rate of helium and tritium from weakly irradiated beryllium pebbles were carried out by means of a Knudsen-cell technique. The samples were heated in a high vacuum to temperatures above the melting point and the evolution of gas release was measured by a mass spectrometer. Different gas diffusion and release stages were recorded and the ruling mechanisms were analysed up to complete exhaustion of the gas inventory. A minor part of the helium content was released by atomic diffusion to free surfaces, starting at about 700 K with a temperature ramp of 10 K/min and about 850 K with 30 K/min. Most of the helium precipitated into bubbles and was released only during abrupt pore venting events, which started at approximately 1500 K. Tritium release was mostly diffusion-dominated. A small fraction of tritium was trapped by helium bubbles during their nucleation phase and was consequently released corresponding to the appearance of the helium peak.

1. Introduction

A key issue of the helium cooled pebble bed (HCPB) tritium breeding blanket for fusion reactors is the behaviour of beryllium pebbles under neutron irradiation and, in particular, retention of helium and tritium and consequent swelling. Gas retention/release and swelling are cumulative effects resulting from complex diffusion phenomena occurring in the solid. These processes must be carefully analysed and modelled; in particular, atomic diffusion, precipitation into bubbles, bubble migration, growth, coalescence and for tritium also solubility, chemical trapping by impurities and surface recombination effects.

Measurements of the release rate of ^{4}He, ^{3}H and ^{3}He (from ^{3}H decay) from irradiated beryllium pebbles were carried out by a Knudsen-cell effusion technique in conjunction with mass spectrometry. A sensitive study of the gas effusion modes was performed over a broad temperature range up to complete release of the gas inventory.

The beryllium samples were fabricated in the USA by Brush Wellman with a fluoride reduction process (FRP), in the form of 2 mm-diameter pebbles. The pebbles, though of a lower quality and with a higher impurity content, have similar shape and microstructure (large grains, 40–200 μm) to the current reference material for the HCPB blanket, i.e. 1 mm-diameter pebbles, produced by NGK in Japan by the rotating electrode process (REP).

The pebbles were irradiated in 1994 in the BERYLLIUM experiment in the high flux reactor in Petten for 97 days. The essential irradiation data are as follows: irradiation temperature 780 K; fast fluence ($E > 0.1$ MeV) 1.24×10^{25} nm^{-2}, 480 appm ^{4}He, about 12 appm ^{3}H in 1994, resulting in about 8 appm ^{3}H and 4 appm ^{3}He in 2001 [1].

2. The experimental technique

A Knudsen-cell facility with a mass spectrometer was used for the measurements of gas release. The furnace

* Corresponding author. Address: Forschungszentrum Karlsruhe, Institute for Nuclear and Energy Technologies, P.O. Box 3640, 76021 Karlsruhe, Germany. Tel.: +49-7247 82 3476; fax: +49-7247 82 4837.
E-mail address: elisa.rabaglino@iket.fzk.de (E. Rabaglino).

0022-3115/02/$ - see front matter
PII: S0022-3115(02)01127-3

can achieve temperatures up to 2500 K and is mounted in a lead-shielded glove box; the scheme of the set-up is shown in Fig. 1. A small tungsten cell (12 mm outer diameter) containing the sample is lifted up into a thermally shielded tungsten heating coil and a ultra-high vacuum of 10^{-6} Pa is created. Gaseous products effuse out through a tiny hole in the top of the cell and a small fraction of the particle beam goes through the ionisation chamber of a quadrupole mass spectrometer located directly above the oven. A liquid-nitrogen loop around the ion source acts as a cold trap for condensable hydrocarbons and rest vapours, so that background noise in the mass spectrometer signal can be significantly reduced. Irradiated beryllium was heated above the melting point ($T_m = 1556$ K [2,3]) with temperature ramps of 10 or 30 K/min, which were obtained by automatic control of the heating resistor voltage. The temperature was measured by a thermocouple inserted in the base of the sample holder. To account for the difference between the temperature measured by the thermocouple and the real temperature of the sample inside the cell, the following calibration procedure was applied: standard samples of silver, zinc, platinum and beryllium were melted and cooled-down: at the freezing point of the sample a thermal arrest occurs at which both temperature and vaporisation rate remain constant for a sufficiently long time, providing fixed points to correct the thermocouple temperature on the basis of the actual melting temperature. After this correction the residual temperature error was less than 5 K.

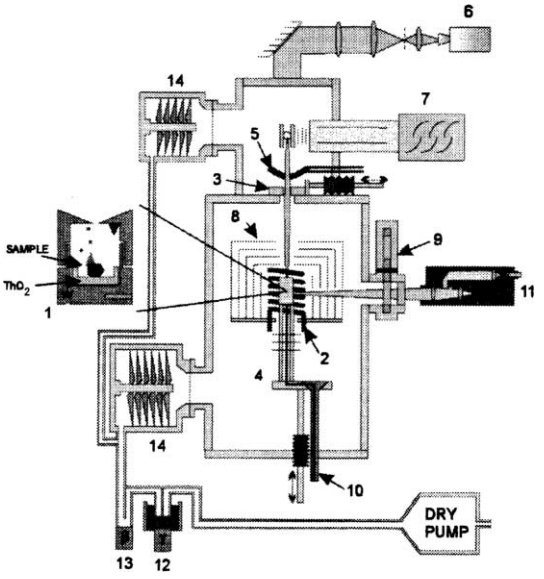

Fig. 1. The Knudsen-cell facility [4]. (1) Knudsen-cell with black-body hole and ThO_2 coating inside; (2) tungsten heating coil; (3) chopper; (4) facilities to move the cell up and down; (5) liquid nitrogen cold trap to reduce background noise; (6) CCD camera to align the cell and the chopper holes; (7) quadrupole mass spectrometer; (8) thermal shields (tungsten/tantalum); (9) pyrometer windows revolver; (10) inlet gas capillary (to introduce purge gases into the cell); (11) linear pyrometer; (12) γ counter with cold trap; (13) β counter; (14) turbo-molecular pumps.

The mass spectrometric detection of ^{9}Be(g) and ^{4}He in the vapour effusing from the irradiated beryllium samples was straightforward, since no isobaric nuclide noise affects their measurement. For ^{4}He, a small contribution of $^{1}H^{3}H$ to mass-4 signal was detected, the ratio $^{3}H/^{4}He$ in the samples being approximately 1.7%. On the other hand, particular care had to be taken in detecting ^{3}H and ^{3}He. In fact, during blank tests, a non-negligible background noise in mass-3 channel was observed, increasing with temperature. This was caused by the presence of relatively large amounts of hydrogen from thermal or electron-induced decomposition of residual hydrocarbons, which in the ion source undergoes the reaction: $H_2^+ + H_2 \rightarrow H_3^+ + H$ [5]. Furthermore, on the basis of the natural abundance of deuterium in hydrogen (0.015%), 0.03% of the hydrogen molecules consist of $^{1}H^{2}H$. Some blank tests were performed in order to study the background noise in mass-3 channel: with the cold trap on, a constant ratio of mass-3 to mass-1 signals was observed (of the order of 0.015, with slight variation). During the tests with irradiated beryllium, the background noise in mass-3 channel could be calculated from the mass-1 signal and was then subtracted.

Further issues in the measurement of tritium arise from its possible appearance in different forms: atomic ^{3}H, di-tritium gas $^{3}H_2$ or protium–tritium $^{1}H^{3}H$. Since the mean free path of atoms in an ultra-high vacuum is longer than the distance between the sample and the mass spectrometer, if tritium leaves the beryllium surface as a single atom, it is very likely detected as a mass-3 atom. Blank tests revealed that no background noise affected mass 6; for ionisation potentials above 30 eV the possible contribution of $^{1}H^{3}H$ to the mass-4 signal was considered to be negligible in view of the much higher ^{4}He inventory in the samples.

In order to verify the appearance of molecular tritium at the beryllium surface and to measure it separately from helium-3, the difference in their first ionisation energy (13.6 eV for hydrogen and 24.6 eV for helium) was considered. Blank tests with increasing ionisation energy in the presence of a helium–hydrogen flow showed that the helium signal clearly appeared above an ionisation energy of 30 eV, whereas only hydrogen was visible at 25 eV. By comparing the gas release curves from irradiated beryllium at 25 and 30 eV, it was possible to isolate the contribution of tritium.

3. Results

Fig. 2(a) shows the measured helium and tritium release rates from irradiated beryllium, with a heating rate of 10 K/min and an ionisation energy of 70 eV. A similar experiment at 25 eV is shown in Fig. 2(b), where hydrogen is detected ($^3H_2$ and $^1H^3H$) but not helium. Fig. 3 shows the effect of a faster heating (30 K/min). Fig. 4 shows the integral release rate for ^{4}He and ^{3}H, normalised with respect to the total inventory, as a function of temperature.

3.1. Helium kinetics

With a temperature ramp of 10 K/min, helium release starts at about 800 K. At higher temperatures, three stages of ^{4}He release can be identified (Fig. 2(a)): (1) atomic diffusion in the range 800–1300 K; (2) precipitation into bubbles in the range 1300–1500 K; (3) bubble venting from 1500 K to $T_m = 1556$ K.

The release of helium measured in the range 800–1500 K is due to the diffusion of helium atoms, initially frozen in the lattice in a dynamical solution, to open

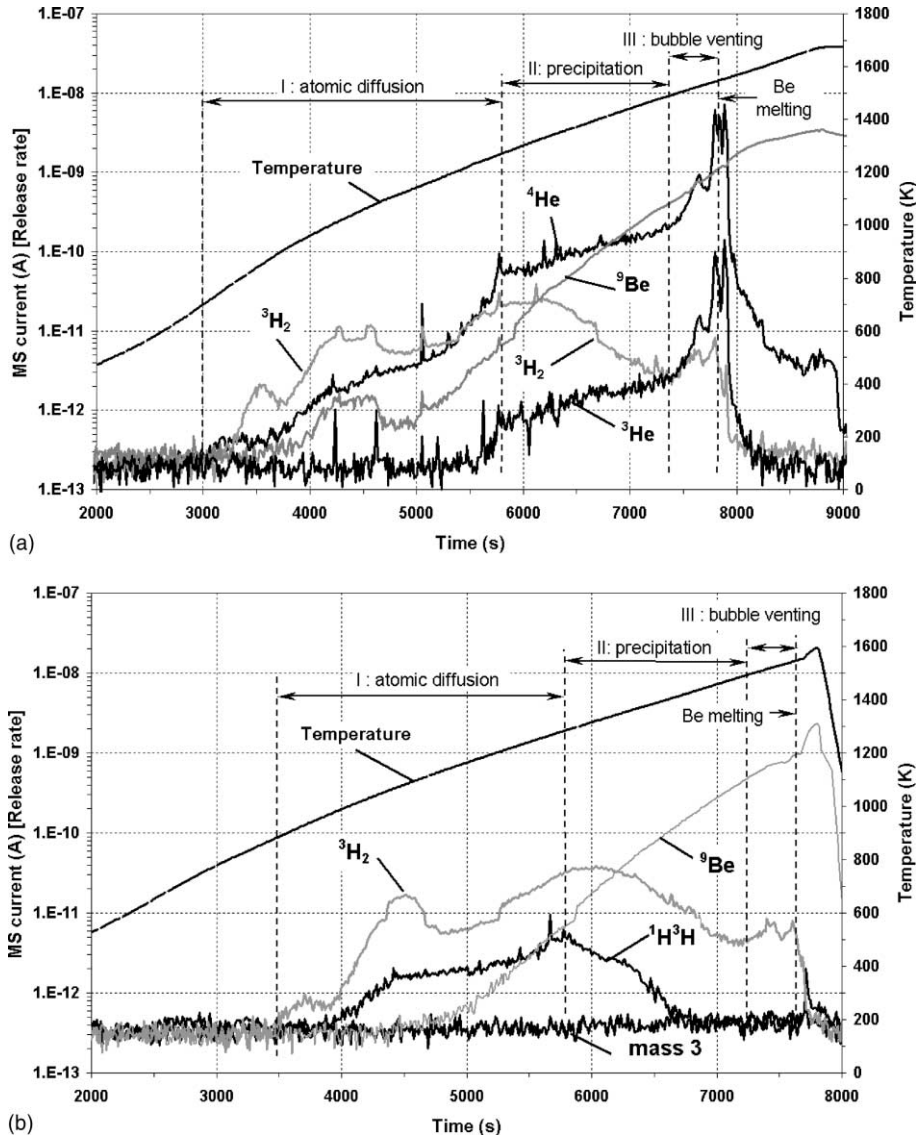

Fig. 2. Helium and tritium release rate from irradiated beryllium pebbles (2 mm-diameter, neutron fast fluence 1.24×10^{25} nm^{-2}, 480 appm ^{4}He, 8 appm ^{3}H and 4 appm ^{3}He) in a vacuum. Temperature ramp: 10 K/min. Ionisation energy: 70 eV (a), 25 eV (b). With 25 eV helium is not detected.

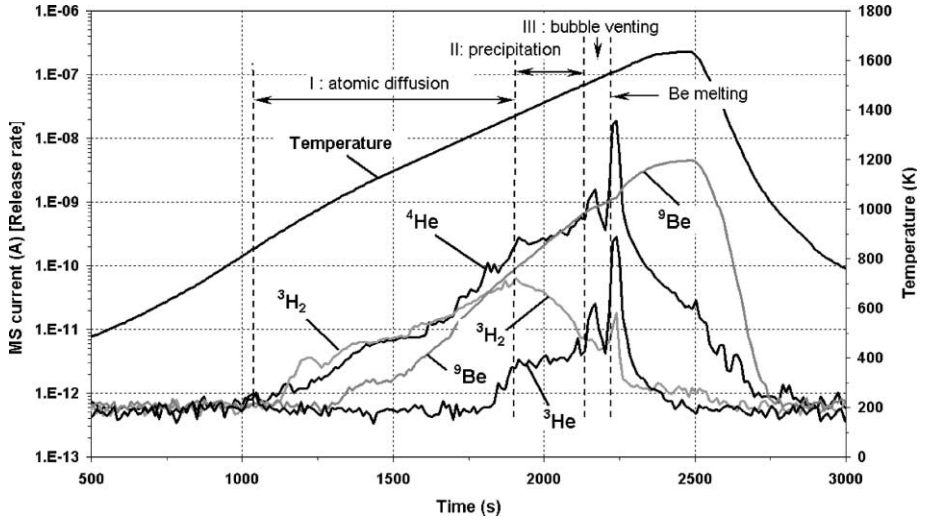

Fig. 3. Helium and tritium release rate from irradiated beryllium pebbles (2 mm-diameter, fast fluence 1.24×10^{25} nm^{-2}, 480 appm ^{4}He, 8 appm ^{3}H and 4 appm ^{3}He) in a vacuum. Temperature ramp: 30 K/min; ionisation energy: 70 eV.

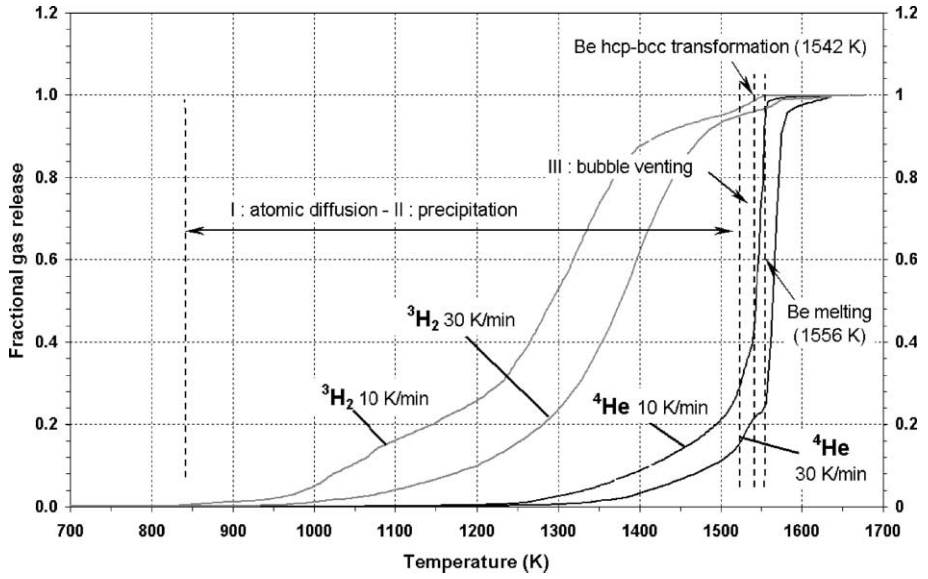

Fig. 4. Integral helium and tritium release from irradiated beryllium pebbles (2 mm-diameter, fast fluence 1.24×10^{25} nm^{-2}, 480 appm ^{4}He, 8 appm ^{3}H and 4 appm ^{3}He) in a vacuum, normalised to the gas inventory.

surfaces, external or internal (mostly intergranular porosity) [6]. At the same time, a consistent part of the gas precipitates into bubbles [7]: the helium trapped in bubbles cannot be released because the time constant for bubble migration to open surfaces is much larger than the duration of the experiment. In the first stage, up to 1300 K, the precipitation is in progress but the diffusion to free surfaces is dominant. Starting from 1300 K, most part of the helium inventory, which was not released, has already precipitated [7] and the remaining helium in the solution begins to exhaust: as a consequence, the release rate curve increases at a lower rate.

Above 1500 K a sharp release peak starts (Figs. 2(a), and 3): in this third stage, approximately 75% of the total initial ^{4}He inventory is released via extensive bubble coalescence and venting, i.e. by a percolation phenomenon [7]. Above ≈1100 K beryllium becomes brittle, so that pressurised pores can easily produce

microcracks (above 1100 K the ultimate tensile strength is <40 MPa) [8]. This release stage crosses first the hcp–bcc phase transition of beryllium (1542 K [2]) and then the melting point (1556 K [2]): during the first phase transition, which involves a large transformation enthalpy (6100 J mol^{-1}, compared to 7200 J mol^{-1} for the melting [2]), there is a strong restructuring of the microstructure and this probably leads to a partial closure of the percolation channels and, consequently, to a temporary arrest of the gas release peak (Figs. 2(a), (b) and 3). A small part of the helium inventory is finally released during melting. Though in these experiments, due to the constant temperature increase, the gas release peak crosses the phase transitions, it starts at lower temperatures (1500 K): this suggests that the percolation mechanisms occur independently. This conclusion is confirmed by the fact that a sharp helium release peak has been observed also by other authors after longer annealing times at constant temperature (1300 K [9], 1120 K [10]) well below the phase transitions.

As far as ^{3}He (from ^{3}H decay) is concerned, the comparison of the mass-3 release rate at an ionisation energy of 70 eV (Fig. 2(a)) and 25 eV (Fig. 2(b)) proves that the mass-3 curve consists essentially of ^{3}He, which was present in a ratio of about 0.8% of ^{4}He. This is verified by the fact that the curves of mass 3 and ^{4}He have a very similar shape. In particular, the reoccurring precipitation and venting stages suggest that ^{4}He and ^{3}He were initially in the same state and that they behave in the same way during the temperature transient.

3.2. Tritium kinetics

Comparison of the release rate of masses 3, 4 and 6 at 70 eV (Fig. 2(a)) and at 25 eV (Fig. 2(b)) proves that tritium is essentially released as di-tritium gas ($^3H_2$, mass 6). A small fraction of tritium combines with protium, giving a negligible contribution to mass 4. No atomic tritium was detected. Since the probability that single tritium atoms combine after leaving the beryllium surface is very low, it can be concluded that most of the tritium was released in a molecular form. Tritium is formed and diffuses in solid beryllium as a single atom, therefore a surface recombination occurs. Effusion of tritium is also influenced by the presence of a thin oxide surface layer and of intragranular precipitates of BeO. At low temperature, tritium can be trapped as $Be(OH)_2$, a compound which decomposes above 600 K. This makes the tritium release modes at low temperature somewhat different from those of helium, but, due to the very low tritium inventory in the samples, this range could not be examined in this study. Starting from 800 K up to 1300–1500 K, tritium release appears to be essentially driven by atomic diffusion, with an exhaustion phenomenon that leads to a decrease of the release rate starting from 1300 K (Fig. 2(a) and (b)). During this phase, helium bubbles capture a small fraction (6%) of tritium (Fig. 4). This fraction is finally released together with helium, as extensive bubble venting takes place at higher temperatures. It can be concluded from these experiments (Fig. 4) that if tritium is not trapped in helium bubbles before the beginning of the heating transient [7], it diffuses out much faster than helium.

If the heating rate is faster (30 K/min, Figs. 3 and 4) the same release stages as by 10 K/min are observed, both for helium and for tritium, but the first diffusion stage starts at higher temperatures (850 K). This is because the same temperature is reached in a shorter time, and the time constants for diffusion are the same. In this case (Fig. 4), though the percolation phase starts at the same temperature as with 10 K/min (1500 K), most part of the helium (78%) is released during melting.

4. Conclusions

Laboratory measurements of helium and tritium release from neutron irradiated beryllium pebbles provided information on the various mechanisms, which affect both the short and long-range migration of these gases. The different release stages occurring in distinct temperature ranges involve both elementary diffusion processes and complex metallographic restructuring of beryllium. Atomic diffusion of helium is accompanied by precipitation into finely dispersed bubbles, which finally coalesce into macroscopic open porosity networks. Only during this restructuring stage a massive release of helium (75% of the inventory) is observed. In the material examined, which is weakly irradiated, most part of the tritium inventory is released by diffusion and only a small part of it (6%) is trapped in helium bubbles during the precipitation phase.

Acknowledgements

The authors would like to thank the staff of the Thermodynamics and Thermophysics Laboratory of the JRC-ITU, in particular F. Capone and J.Y. Colle, who performed the experiments, and P. Damen for the support and useful discussions. A special thank to Dr H. Kleykamp for his valuable suggestions and to R. Drummond for the corrections of the English language.

References

[1] R. Conrad, R. May, BERYLLIUM final irradiation report, EC-JRC-IAM Report P/F1/96/15, 1996.
[2] H. Kleykamp, Therm. Acta 345 (2000) 179.
[3] Gmelin Handbook of Inorganic and Organometallic Chemistry, Be Suppl., Vol. A2, Springer-Verlag, Berlin, 1991.

[4] F. Capone, Y. Colle, J.P. Hiernaut, C. Ronchi, J. Phys. Chem. A 103 (1999) 10899.
[5] A.L. Sessions, T.W. Burgoyne, J.M. Hayes, Anal. Chem. 73 (2001) 192.
[6] F. Capone, J.P. Hiernaut, M. Martellenghi, C. Ronchi, Nucl. Sci. Eng. 124 (1996) 436.
[7] E. Rabaglino, C. Ferrero, J. Reimann, C. Ronchi, T. Schulenberg, in: Proceedings of 6th International Symposium on Fusion Nuclear Technology, San Diego, Fusion Engineering and Design, in press.
[8] A.S. Pokrovsky, S.A. Fabritsiev, R.M. Bagautdinov, Yu. Goncharenko, J. Nucl. Mater. 233–237 (1996) 841.
[9] F. Scaffidi-Argentina, Fus. Eng. Des. 58&59 (2001) 641.
[10] F. Scaffidi-Argentina, H. Werle, in: Proceedings of 2nd IEA International Workshop on Beryllium Technology for Fusion, Jackson Lake Lodge, Wyoming, USA, 1995.